

Modeling CO₂ laser ablation impulse of polymers in vapor and plasma regimes

John E. Sinko (新光ジョンエリフ)^{1,a)} and Claude R. Phipps²

¹Micro-Nano Global Center of Excellence, Graduate School of Engineering, Nagoya University, Furo-cho, Chikusa-ku, Nagoya 464-8603, Japan

²Photonic Associates LLC, 200A Ojo de la Vaca Road, Santa Fe, New Mexico 87508, USA

(Received 5 April 2009; accepted 31 August 2009; published online 28 September 2009)

An improved model for CO₂ laser ablation impulse in polyoxymethylene and similar polymers is presented that describes the transition effects from the onset of vaporization to the plasma regime in a continuous fashion. Several predictions are made for ablation behavior. © 2009 American Institute of Physics. [doi:10.1063/1.3234382]

A model has been needed to predict thrust and specific impulse (I_{sp}) over the likely parameter range of laser space propulsion. In earlier works, e.g., Pirri¹ developed laser-surface interaction theory primarily as an aerodynamic problem for the vapor regime in atmosphere with some connection to the plasma regime. Phipps *et al.*² addressed vacuum ambient with a treatment that permitted ablation pressure predictions within a factor of 2 over an extremely broad range $100 \text{ ps} < \tau < 1 \text{ ms}$, $0.25 \text{ }\mu\text{m} < \lambda < 10.6 \text{ }\mu\text{m}$, but with intensity limits excluding inertial confinement fusion (ICF) extremes and very short pulses.³ The theory of Lindl⁴ covers the ICF regime. Previous models^{5,6} treated plasma and vapor regimes separately. A simple, fluence-dependent impulse model was missing for field applications (e.g., laser plasma thrusters or space debris removal⁷) allowing a smooth transition between regimes. This paper proposes such a bridge.

The momentum coupling coefficient C_m is the ratio of laser ablation impulse density σ to incident laser pulse fluence Φ (or pressure p to intensity I for continuous lasers). Using the ablated mass areal density μ (kg/m²) and exhaust velocity v_E (m/s), $\sigma = \mu \times v_E$, where $v_E = \langle v_x \rangle$ is the first moment of the velocity distribution $f(v_x)$ along the thrust axis x . The velocity distribution is often a “drift Maxwellian,”⁸

$$C_m = \sigma/\Phi \approx p/I \quad (\text{N s/J}) \quad \text{or} \quad (\text{N/W}). \quad (1)$$

The specific impulse I_{sp} , used in rocket engineering, is related to v_E by

$$I_{sp} \approx v_E/g_o = Mv_E/(Mg_o) = \sigma/(\mu g_o) \quad (\text{s}). \quad (2)$$

I_{sp} originally represented the impulse from a unit *weight* of a fuel mass M on the launch pad at sea level. In the modern definition of I_{sp} , g_o is a constant with no physical meaning. It is accepted practice to apply I_{sp} (with $g_o=9.8$) to space systems that never operate on the Earth’s surface. The ablation efficiency η_{AB} is the efficiency with which incident laser pulse energy is converted into exhaust kinetic energy:

$$\begin{aligned} \eta_{AB} &= \mu \psi v_E^2 / (2\Phi) \\ &= \psi C_m v_E / 2 = (\psi g_o / 2) \times C_m I_{sp}, \end{aligned} \quad (3)$$

where in Maxwellian plasmas

$$\psi = \frac{\langle v_x^2 \rangle}{(\langle v_x \rangle)^2} = \left\{ \frac{v_E^2 + kT_e/m_e}{v_E^2} \right\}. \quad (4)$$

For typical ablation plume shapes, $1 < \psi \leq 1.15$,⁹ and use of $\psi \approx 1$ is typical (this underestimates η_{AB}). For clarity, this assumption will also be used here. There are only three cases where $\eta_{AB} > 1$: chemical reaction of the target with its ambient atmosphere (e.g., combustion in air); if the ablation process is exothermic;⁶ and for confinement geometries, where the target geometry or ambient atmosphere restrict the expansion of ablation products, increasing the interaction time between the exhaust and the vehicle. These cases are not mutually exclusive.

At intensities sufficient for fully ionized plasma, absorption is by inverse Bremsstrahlung (IB). One-dimensional thermal transport theory¹⁰ predicts that surface temperature T varies with time (here, laser pulse length τ) as

$$T(\tau) = [2I_o \times (\kappa\tau/\pi)^{1/2}] / K \quad (\text{K}), \quad (5)$$

where I_o is the ablation threshold in W/m², and κ and K are the thermal diffusivity and thermal conductivity, respectively. Data in Fig. 1 shows that for plasma ignition, $I \times \tau^{1/2}$ is constant. Plasma density increases with temperature until the “critical density” of electrons n_{ec} is reached

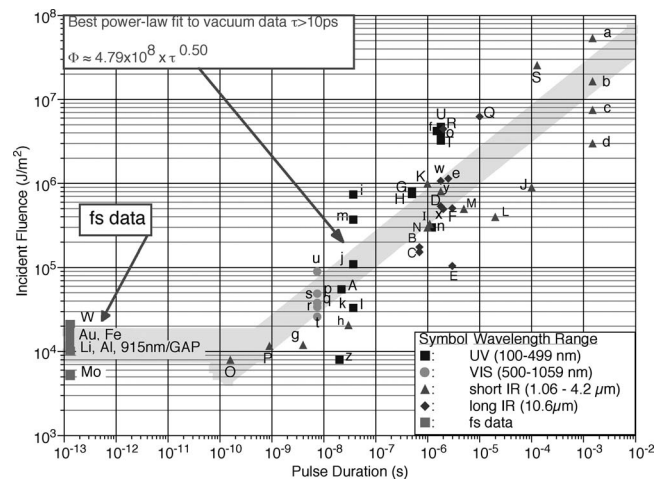


FIG. 1. Fluence required for plasma ignition on targets in vacuum from 100 fs to 1 ms pulse duration: $\Phi \sim I \times \tau^{0.5}$. This plot shows that less pulse energy is required to form plasma as τ decreases, down to about 100 ps. Data labels are explained in Refs. 11 and 12.

^{a)}Electronic mail: sinko@fuji.nuae.nagoya-u.ac.jp.

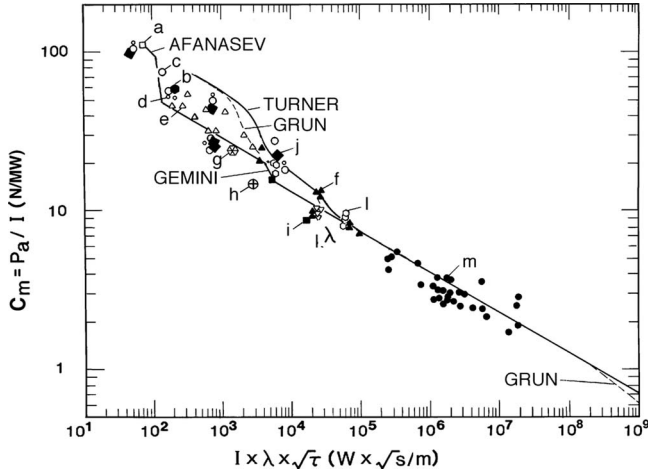


FIG. 2. Plasma model fitting of published data for C_m on C-H materials, adapted from Ref. 2. Four data subsets were used with distinct Saha equations, including short pulses in UV (Turner, 248 nm, 22 ns) and near IR (Grun, 1.06 μm , 5 ns); and long pulses in near IR (Afanasev, 1.06 μm , 1.5 ms) and mid IR (Gemini, 10.6 μm , 1.8 μs). Fitting curves are given for each data set. Names and data labels are explained in Ref. 2.

$$n_{ec} = m_e n_e^2 \omega^2 / (4\pi e^2) \approx 1.115 \times 10^{27} / \lambda_{\mu\text{m}}^2 \text{ (m}^{-3}\text{)}, \quad (6)$$

where m_e , n_e , and e are respectively the mass, number density, and charge of the electron and ω is the laser frequency ($\omega = 2\pi c / \lambda$). The Saha equation¹¹ gives relative densities of the i th and $(i-1)$ th ionization states

$$\frac{n_e n_i}{n_{i-1}} = \frac{2u_i}{u_{i-1}} \left(\frac{2\pi A m_p k T_e}{h^2} \right)^{3/2} \times e^{-W_{i,i-1}/(kT_e)}, \quad (7)$$

using the proton mass m_p , the atomic number A , Boltzmann's constant k , the electron temperature T_e , Planck's constant h , and the ionization energy $W_{i,i-1}$ between the i th and $(i-1)$ th states. The number densities and quantum-mechanical partition functions of the i th and $(i-1)$ th states are given by n_i and n_{i-1} ; and u_i and u_{i-1} , respectively. If only one ionization state is present, the ionization fraction reduces to $\eta_i = 2 \times n_e / (n_o + 2 \times n_e)$, since $n_i + n_e = 2 \times n_e$ for single stage ionization. If p is the total pressure of all species

$$B_{\text{Saha}} = \frac{2u_1}{u_0} \times \left(\frac{2\pi m_e k T_e}{h^2} \right)^{3/2}, \quad (8)$$

$$n_e = B_{\text{Saha}} e^{-W_{i,i-1}/(kT_e)} \left(\sqrt{1 + \frac{p}{kT_e B_{\text{Saha}}} e^{-W_{i,i-1}/(kT_e)}} - 1 \right) \approx \sqrt{n_0 B_{\text{Saha}}} e^{-W_{i,i-1}/(kT_e)}. \quad (9)$$

In a study of vapor-plasma transitions, Eq. (9) applies. Phipps *et al.*² derived Eqs. (10) and (11) for $i \geq 1$,

$$C_m = (1.84 \times 10^{-4}) \frac{\Psi^{9/16}}{A^{1/8} (I \lambda \sqrt{\tau})^{1/4}} \text{ (N/W)}, \quad (10)$$

$$I_{\text{sp}} = 442 \frac{A^{1/8}}{\Psi^{9/16}} (I \lambda \sqrt{\tau})^{1/4} \text{ (s)}, \quad (11)$$

where $\Psi = A / \{2 \times [Z^2 \times (Z+1)]^{1/3}\}$, A is the average atomic mass number, and Z is the average state of ionization (≥ 1) of atoms in the (fully ionized) plasma. Figure 2 shows several fitting curves of the model to different published data in the plasma regime, using Eqs. (10) and (11).^{12,13} However, it

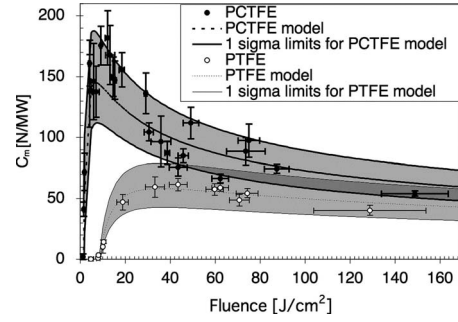


FIG. 3. Equation (14) predicts pulsed CO₂ laser ablation below and perhaps slightly into the plasma regime. Each point is averaged from 5 to 10 shots, and $\pm 1\sigma_s$ parameter estimates from modeling and $\pm 1\sigma_s$ experimental error bars are included (σ_s is one standard deviation).

is clear that, in Eq. (10), $\lim_{\Phi \rightarrow 0} (C_m) \rightarrow \infty$, whereas actually $\lim_{\Phi \rightarrow 0} (C_m) = 0$, so a model for low intensity is needed.

At low fluence, vaporization drives impulse generation. The incident laser pulse energy is reduced by reflectivity at the target surface and by deposition into the target (and exhaust) that does not contribute to exhaust kinetic energy. Reflectivity follows the Fresnel relations,¹⁴ dependant on the surface condition and refractive index at the ablation wavelength. It has been established by many authors (e.g., Anisimov and Khokhlov,¹⁵ Bäuerle,¹⁶ Ready,¹⁷ and Srinivisan *et al.*¹⁸) that the ablation mechanism evolves from thermal to optical as the ablating wavelength decreases. For ablation of CHO (organic) materials like polymers, thermal diffusion is usually negligible at ultraviolet (UV) wavelengths, but energy deposition can be described as photochemical even at longer wavelengths.¹⁶ Following Srinivisan *et al.*¹⁸ we assume the Bouguer–Lambert–Beer absorption law¹⁹ governs energy deposition. The actual dependence is influenced by, e.g., thermal effects and the laser beam spatial profile. We tested several models against low-fluence polymer ablation data and found that a pure photochemical model exhibited the best fit. Furthermore, theoretical predictions of the ablation threshold^{15–17} that rely on latent heat of vaporization are inconsistent with experimental data on CO₂ laser ablation of polymer polyoxymethylene (POM) targets.^{20–22} For CO₂ lasers with long pulse lengths, the characteristic photochemical and photothermal length scales can be of the same order, but inclusion of photothermal effects only inhibited modeling and analysis. Assuming photochemical absorption of infrared

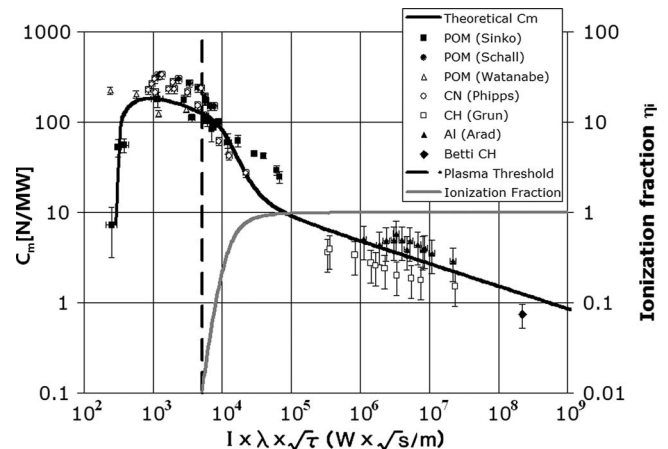


FIG. 4. A combined model for C_m , showing fit to data from vaporization onset into the plasma regime.

(IR) radiation in the polymer, the areal ablated mass density μ is:

$$\mu = (\rho/\alpha) \times \ln(C\Phi/\Phi_o) \quad (\text{kg/m}^2), \quad (12)$$

where Φ_o is the critical threshold fluence for vaporization of the target, ρ is its density, and C is a parameter indicating multiplicative energy losses, e.g., reflectivity, exhaust divergence effects, and exhaust energetic modes that do not contribute to propulsion. Φ_o includes subtractive energy losses such as heating of unvaporized target material and energy necessary for vaporization of the exhaust.¹⁵⁻¹⁷ Using energy conservation, the momentum areal density $[\sigma]$ is:

$$\sigma^2/(2\mu) = C\Phi - \Phi_o = \Phi_o(\xi - 1), \quad (13)$$

where $\xi = C \times \Phi/\Phi_o$. Then, C_m and I_{sp} are

$$C_m = \sqrt{\frac{2\rho C^2}{\alpha\Phi_o}} \times \frac{\xi - 1}{\xi^2} \times \ln \xi \quad (\text{Ns/J}), \quad (14)$$

$$I_{sp} = \sqrt{\frac{2\alpha\Phi_o}{\rho g_o^2}} \times \frac{\xi - 1}{\ln \xi} \quad (\text{s}). \quad (15)$$

$$\eta_{AB} = (g_o/2)C_m I_{sp} = C(\xi - 1)/\xi. \quad (16)$$

Equation (16) implies that $\lim_{\xi \rightarrow \infty}(\eta_{AB}) = C$ and that $\lim_{\xi \rightarrow 1}(\eta_{AB}) = 0$. Figure 3 shows the success of this model.

The proposed solution distinguishes between (neutral) vaporized and plasma species, analogous to a two-fluid model. Our treatment, supported by the spatial separation of the vaporization and plasma absorption processes, uses conservation of energy to form two impulse terms. At low fluence, most of the energy of the laser pulse reaches the surface and imparts impulse via vaporization, while at high fluence, most of the pulse energy is instead absorbed via IB above the surface, imparting impulse to the target via plasma pressure. The transition from transparent vapor to absorbing plasma occurs within a relatively narrow range of fluence, so effects from partial ionization, although interesting, may be neglected in favor of simplicity without significantly impairing the model. In approximation, the IB absorption coefficient is related to the ionization fraction by $\alpha_{IB} \sim \eta_i^2$. Neglecting interaction terms, approximating the transmission factor for vaporization impulse to first order, and denoting by C_{mp} and C_{mv} the coupling coefficients from Eqs. (10) and (14), respectively, Eq. (17) provides a reasonable mechanism for smoothly connecting the two models

$$C_m = \eta_i C_{mp} + (1 - \eta_i) C_{mv}. \quad (17)$$

This expression provides a means for calculating C_m over the entire intensity range from ablation onset into the plasma regime. Figure 4^{2,20-26} shows the success of this treatment for POM and similar materials under CO₂ laser irradiation. AI can be included in Fig. 4 because the data are only from the plasma regime, where an argument about photochemistry is moot.

Maximization of (14) yields a single solution.²⁷ A different expression is found by maximizing the Phipps vaporization model⁵ as shown in Table I. The solutions are not arbitrary “fitting factors” but rather mathematically derived constants characteristic of the chosen models. This treatment introduces an intriguing method for testing laser ablation im-

TABLE I. Predictions for optimal coupling at low fluence.

	Phipps	Sinko
Transcendental equation	$\xi = [2(\ln \xi)^2 - 1]/(\ln \xi - 1)$	$\ln \xi = (\xi - 1)/(\xi - 2)$
Solution (J/cm ²)	$\Phi_{\text{opt}} \approx 6.9 \times \Phi_o$	$\Phi_{\text{opt}} \approx 4.2 \times \Phi_o$

pulse models, since the fluence for maximal C_m and threshold fluence can be validated experimentally. In this work, both models have critical points at $\xi = 1$ that are not maximal, representing the ablation threshold. In real systems, the ablation threshold is more complex; however, very low fluence effects at the threshold are not pertinent to the present treatment, which focuses on significant impulse generation by ablation of the target. The predictions for Φ_{opt} should apply (approximately) in the connected model; however, the analytical results may be at variance with real ablation data, due to, e.g., thermal diffusion and plasma effects. The predictions are already testable using literature data.

¹A. N. Pirri, *Phys. Fluids* **16**, 1435 (1973).

²C. R. Phipps, Jr., T. P. Turner, R. F. Harrison, G. W. York, W. Z. Osborne, G. K. Anderson, X. F. Corlis, L. C. Haynes, H. S. Steele, K. C. Spicchi, and T. R. King, *J. Appl. Phys.* **64**, 1083 (1988).

³J. Ihlemann, F. Beinhorn, H. Schmidt, K. Luther, and J. Troe, *Proc. SPIE* **5448**, 572 (2004).

⁴J. Lindl, *Phys. Plasmas* **2**, 3933 (1995).

⁵C. R. Phipps, Jr., R. F. Harrison, T. Shimada, G. W. York, T. P. Turner, X. F. Corlis, H. S. Steele, L. C. Haynes, and T. R. King, *Laser Part. Beams* **8**, 281 (1990).

⁶C. R. Phipps, J. Luke, and T. Lippert, *Thin Solid Films* **453**, 573 (2004).

⁷C. R. Phipps, H. Friedman, D. Gavel, J. Murray, G. Albrecht, E. V. George, C. Ho, W. Priedhorsky, M. M. Michaelis, and J. P. Reilly, *Laser Part. Beams* **14**, 1 (1996).

⁸R. Kelly and R. Dreyfus, *Nucl. Instrum. Methods Phys. Res. B* **32**, 341 (1988).

⁹C. Phipps and M. Michaelis, *Laser Part. Beams* **12**, 23 (1994).

¹⁰H. Carslaw and J. Jaeger, *Conduction of Heat in Solids* (Clarendon, Oxford, 1959), p. 75.

¹¹M. Saha, *Philos. Mag.* **40**, 472 (1920).

¹²C. Phipps, J. Luke, D. Moore, J. Glowina, and T. Lippert, *Appl. Surf. Sci.* **252**, 4838 (2006).

¹³C. R. Phipps and J. Luke, *AIAA J.* **40**, 310 (2002).

¹⁴M. Born and E. Wolf, *Principles of Optics*, 7th ed. (Cambridge University Press, Cambridge, 1999), Chap. 1.5, pp. 42–43.

¹⁵S. I. Anisimov and V. A. Khokhlov, *Instabilities in Laser-Matter Interaction* (CRC, Boca Raton, 1995).

¹⁶D. Bäuerle, *Laser Processing in Chemistry*, 3rd ed. (Springer, Berlin, 2000).

¹⁷J. F. Ready, *Effects of High-Power Laser Radiation* (Academic, New York, 1971).

¹⁸V. Srinivisan, M. A. Smrtic, and S. V. Babu, *J. Appl. Phys.* **59**, 3861 (1986).

¹⁹J. E. Stewart, *Infrared Spectroscopy: Experimental Methods and Techniques* (Marcel Dekker, Inc., New York, 1970), Chap. 3, p. 82.

²⁰J. E. Sinko, “Vaporization and Shock Wave Dynamics for Impulse Generation in Laser Propulsion,” Ph.D. thesis, The University of Alabama in Huntsville, 2008.

²¹W. O. Schall, H.-A. Eckel, J. Tegel, F. Waiblinger, and S. Walther, “Properties of Laser Ablation Products of Delrin with CO₂ Laser,” EOARD Report No. FA8655-03-1-3061, 2004.

²²K. Watanabe, K. Mori, and A. Sasoh, *J. Propul. Power* **22**, 1148 (2006).

²³R. Betti, personal communication (2008).

²⁴J. Sinko and A. Pakhomov, *AIP Conf. Proc.* **997**, 254 (2008).

²⁵J. Grun, S. Obenschain, B. Ripin, R. Whitlock, E. McLean, J. Gardner, M. Herbst, and J. Stamper, *Phys. Fluids* **26**, 588 (1983).

²⁶B. Arad, S. Eliezer, Y. Gazit, H. Loebenstein, A. Zigler, H. Zmora, and S. Zweigenbaum, *J. Appl. Phys.* **50**, 6817 (1979).

²⁷J. E. Sinko and D. A. Gregory, *Proc. SPIE* **7005**, 70052Q (2008).